Polymer Journal (2021) 53:1073–1082
https://doi.org/10.1038/s41428-021-00505-y

FOCUS REVIEW

Rheological studies on polymer networks with static and dynamic crosslinks

Takuya Katashima[1]

Received: 24 March 2021 / Revised: 5 May 2021 / Accepted: 8 May 2021 / Published online: 11 June 2021
© The Society of Polymer Science, Japan 2021

Abstract

The three-dimensional structures of polymer networks are formed through two types of crosslinks: static and dynamic. Although the characteristics of crosslinks strongly influence the rheological properties of polymer networks, the understanding of the molecular origin of these properties remains incomplete owing to structural complexity. The relationship between the structure and dynamics of polymer networks and their rheological behavior can be elucidated based on multiple experimental methods. From this viewpoint, this review introduces rheological studies on static and dynamic polymer networks. Investigations of the nonlinear elastic behaviors of model static networks (Tetra gels) through general biaxial stretching revealed that a cross-effect of strains in different directions is present, even in networks without defects, which is not considered in conventional molecular models. Linear viscoelastic and spectroscopic studies on dynamic networks (host–guest gels and hydrophobically modified ethoxylated urethane) have shown that conventional molecular models are not suitable for describing rheological properties. Dynamic heterogeneities, such as the different mobilities of rotaxane-like crosslinks and micelles, strongly influence the rheological properties. These results demonstrate the remaining issues to be investigated to obtain a molecular understanding of the rheological properties of polymer networks.

Introduction

The physical properties of polymeric materials are strongly correlated with their structures and dynamics. The three-dimensional structures of polymer networks are formed by crosslinking one-dimensional polymer chains. These complex structures impart polymer networks with various characteristics, such as a nonlinear elastic response, robustness, and viscoelasticity. In general, network structures are primarily determined by the polymer concentration, the molar mass between the crosslinks, and the number density of the crosslinks.

There are two main types of crosslinks: (i) stable bonds such as covalent bonds and microcrystals and (ii) unstable and noncovalent bonds, such as hydrogen bonds and ionic bonds. The binding energy of the former crosslinks is greater than the thermal fluctuations (at least at a desired temperature), resulting in a permanent crosslinking structure called a static network. The latter crosslinks undergo repeated association and dissociation driven by thermal fluctuations, forming a dynamic network. The stability of the crosslinking structures determines the physical properties of the polymer networks.

Polymer network materials exhibit complex rheological behaviors, including viscoelasticity, which allow them to be utilized for tires and other applications. They are also used in drug delivery systems and electrophoresis because of their ability to retain substances in the network and because of their molecular sieving properties. In recent years, many studies have been carried out to investigate the design of tough hydrogels [1–4] and self-healable gels [5–11] by controlling the crosslinking structures. In some tough hydrogels, a mechanism for dissipating applied stress is incorporated not only by controlling the static network structure but also by including dynamic networks through the introduction of sacrificial bonds [12–18] or movable crosslinks [19–22].

However, the relationship between the structure and dynamics of polymer networks and their rheological behavior is not entirely understood. One reason is that unexpected structures such as spatial and connective heterogeneities are

---

✉ Takuya Katashima
katashima@tetrapod.t.u-tokyo.ac.jp

[1] Department of Bioengineering, School of Engineering, The University of Tokyo, 7-3-1 Hongo, Bunkyo-ku, Tokyo, Japan

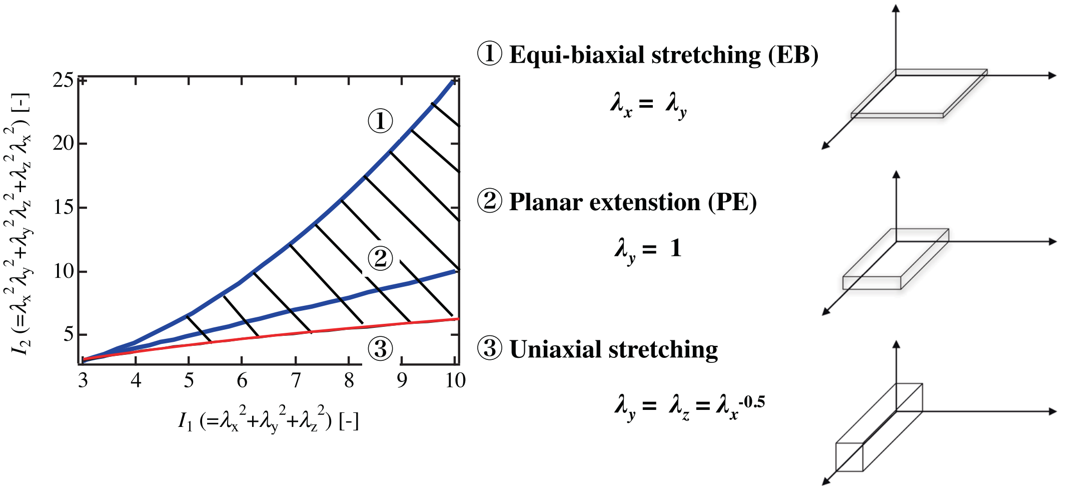

Fig. 1 General biaxial deformations of incompressible materials and physically accessible deformations (shaded area) as functions of I_1 and I_2

inevitably introduced into polymer networks [23], which are impossible to detect and control precisely. The other reason is that limited experimental approaches have been used to establish and verify molecular models, which has led to an inaccurate understanding. Thus, a deeper understanding of rheological properties such as high deformability and self-healing should be obtained by investigating the dynamics and structures of various systems using complex experimental methods.

This review presents recent studies on the relationship between polymer network materials with static and dynamic crosslinking structures and their rheological properties, which the author has studied. First, the large deformation behavior of Tetra gels with homogeneous network structures, as representative static networks, is presented. The behavior under multiaxial deformation is compared with molecular models, and new findings are introduced. Second, the viscoelastic properties and diffusivity of dynamic networks, as represented by host–guest (HG) gels and hydrophobically modified ethoxylated urethane (HEUR), are comprehensively evaluated.

Rheological properties of polymer networks with static crosslinking

One of the characteristics of static polymer networks is their remarkable nonlinear elasticity. Compared with metals and ceramics, static polymer networks, such as elastomers and gels, exhibit a nonlinear stress–strain relationship, even in the elastic region. The stress–strain relationship is governed by the strain energy density (W) function because the nominal stress (σ_i) is the partial derivative of W with respect to the elongation rate (λ_i) in the i-axis direction. Over the last half-century, many W functions have been proposed for polymer networks with various network structures. However, the understanding of the relationship between W and network structures remains incomplete for two main reasons. First, the deformation range of conventional mechanical tests is limited. In general, the W function has been experimentally estimated using stretching and compression tests. Figure 1 shows the relationship between the first and second invariants of Green's deformation tensor ($I_1 = \lambda_x^2 + \lambda_y^2 + \lambda_z^2$ and $I_2 = \lambda_x^2\lambda_y^2 + \lambda_y^2\lambda_z^2 + \lambda_z^2\lambda_x^2$). The shaded area corresponds to the physically accessible region of an incompressible material ($\lambda_x^2\lambda_y^2\lambda_z^2 = 1$). As uniaxial deformation is a special case of physically accessible deformation, it provides a limited basis for discussing the W function. Many studies have reported that the W function estimated from stretching tests cannot explain the stress–strain relationship for other types of deformation. Second, static network structures are generally uncontrollable and inevitably contain heterogeneities in spatial arrangements (nonuniform distributions of crosslinks) and connectivity (dangling, elastically ineffective loop structures). Such uncontrollable heterogeneities lead to inaccurate estimates of structural parameters (molar mass of network strands, density of crosslinks, etc.). Furthermore, previous studies have used elastomers that contain entanglements. The presence of trapped entanglements in an elastomeric network has been considered the main reason for deviations of the stress–strain behavior from the predictions of the classical neo-Hookean (NH) model for ideal polymer networks without structural defects. However, there is no approach to estimate W for real polymer networks without structural defects because the corresponding samples have not yet been synthesized. Such a system would provide an essential basis for understanding the rubber elasticity of most real networks with complex structures.

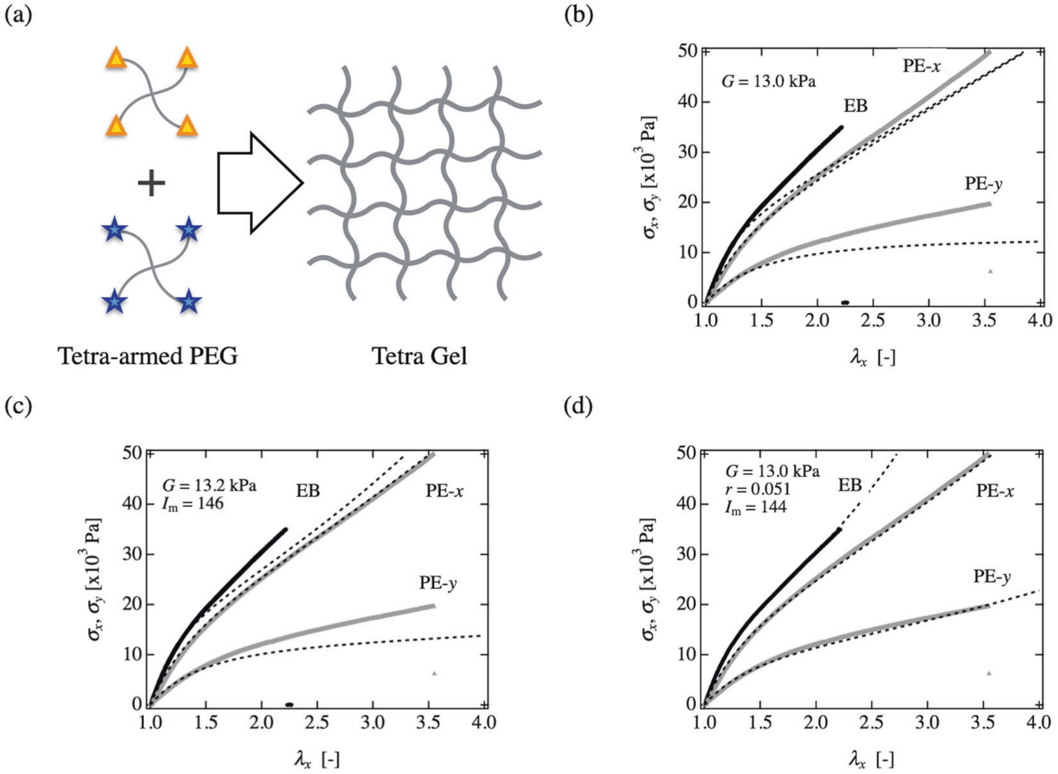

Fig. 2 **a** Schematic illustration of a Tetra gel. **b** Nominal stress as a function of the stretching ratio in the *x*-direction for a Tetra gel under equibiaxial stretching and planar extension. The dashed lines represent the predictions of the NH model. **c** Comparison with the Gent model. **d** Comparison with the extended Gent model. Reproduced from [24] by permission of the Royal Society of Chemistry

In 2008, Sakai et al. improved the model network system and created a “Tetra gel” corresponding to an ideal or near-ideal network (Fig. 2a) [3]. Tetra gels are formed by AB-type crosslinks between two mutually reactive four-armed polyethylene glycols (PEGs). Many experiments have shown that Tetra gels have less heterogeneity and better structural controllability than conventional model networks [23]. Subsequently, the biaxial stretching of Tetra gels was investigated. The observed behavior was compared to the conventional *W* function represented by the NH model, and deviations from the traditional molecular understanding were discussed [21, 24].

Figure 2b shows the results for the biaxial stretching of a Tetra gel. The polymer volume fraction in the as-prepared state (φ_0) was 0.096, which corresponds to approximately twice the concentration required to achieve overlap between precursor chains. The applicability of the NH model to biaxial data was verified. The *W* function of the NH model is expressed as [25]:

$$W = \frac{G}{2}(I_1 - 3) = \frac{G}{2}\left(\lambda_x^2 + \lambda_y^2 + \lambda_z^2 - 3\right) \qquad (1)$$

Here, *G* and λ_i are the shear modulus and the elongation ratio in the *i* direction ($i = x$, y, and z), respectively. This function includes only I_1 as a variable. The stress–strain relationships for each deformation mode using the NH model are given by:

$$\sigma_{EB} = G\left(\lambda_x - \lambda_x^{-5}\right) \qquad (2)$$

$$\sigma_{PE-x} = G\left(\lambda_x - \lambda_x^{-3}\right) \qquad (3)$$

$$\sigma_{PE-y} = G\left(1 - \lambda_x^{-2}\right) \qquad (4)$$

where the condition of isovolumetric deformation ($\lambda_x\lambda_y\lambda_z = 1$) is employed. The NH model has been considered suitable for ideal polymer networks with infinite extensibility and without structural defects. The dashed lines in Fig. 2b represent the stress–elongation relationships given by Eqs. (2)–(4). Although a satisfactory fit is obtained in the small strain region, the NH model deviates downward from the experimental data at a moderate deformation of $\lambda_x > 1.3$. Thus, the stress–elongation behaviors of the Tetra gel, which was assumed to be an ideal network, differ considerably from those predicted by the NH model. This deviation is expected to originate primarily from the absence of finite extensibility for the network strands. Conventionally, strain hardening in a large deformation region is modeled using the non-Gaussian statistics for strongly stretched chains. Here, the Gent model was

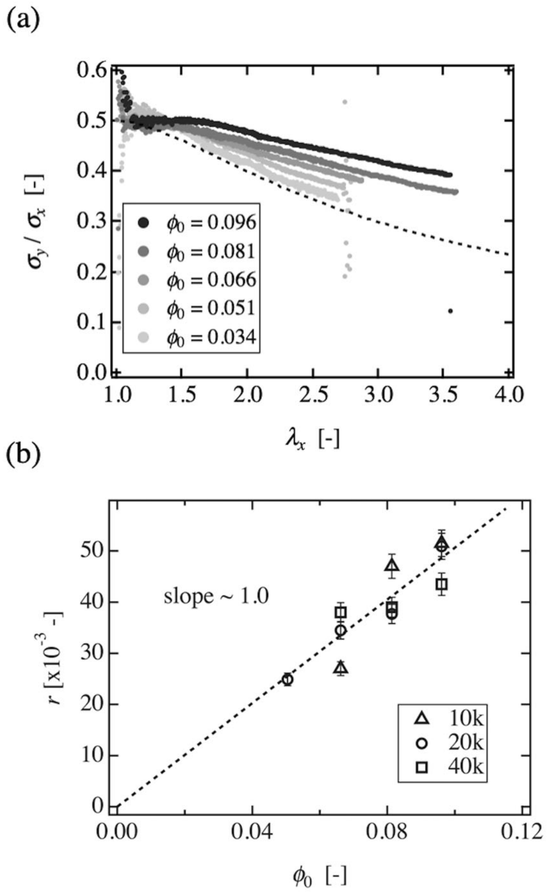

Fig. 3 **a** Stress ratio (σ_y/σ_x) as a function of the stretching ratio in the x-direction under planar extension for various Tetra gel samples. The dashed line shows the prediction of Eq. (9). **b** r as a function of φ_0 for Tetra gels with various precursor chain lengths. Reproduced from [24] and [21] by permission of the Royal Society of Chemistry and the American Institute of Physics, respectively

adopted [26], which describes finite extensibility using a minimal addition to the NH model. The elastic free energy of the Gent model is expressed as:

$$W = -\frac{G}{2}(I_m - 3)\ln\left(1 - \frac{I_1 - 3}{I_m - 3}\right) \tag{5}$$

where I_m is the maximum value of I_1, at which the stress becomes infinite. The dashed lines in Fig. 2c show the predictions of this gradient model. Compared with the NH model, the reproducibility of this model is improved, but obvious deviations from the experimental data remain. The deviation is especially significant in the y-direction under planar deformation, which means that the cross-effect of the strain in one direction on the stress in the other direction is stronger than theoretically predicted.

Figure 3a shows the stress ratio $\sigma_{\text{PE-}x}/\sigma_{\text{PE-}y}$ against λ_x for various Tetra gel samples. The observed decrease in $\sigma_{\text{PE-}x}/\sigma_{\text{PE-}y}$ with increasing λ_x becomes more pronounced as φ_0 decreases. The stress ratio under planar extension is a measure of the cross-effect of strains in different directions on stress. In general, the W function for incompressible materials ($\lambda_x\lambda_y\lambda_z = 1$) is expressed as a function of I_1 and I_2. The stresses in biaxial deformation are given by:

$$\sigma_i = \frac{\partial W}{\partial \lambda_i} = \frac{2}{\lambda_i}\left(\lambda_i^2 - \frac{1}{\lambda_i^2\lambda_j^2}\right)\left(W_1 + \lambda_j^2 W_2\right) \tag{6}$$

where W_1 and W_2 represent the derivatives of W with respect to I_1 and I_2, respectively. Eq. (7) provides a general expression for the stress ratio under planar extension:

$$\frac{\sigma_y}{\sigma_x} = \frac{\lambda_x}{\lambda_x^2 + 1} + AW_2 \tag{7}$$

where

$$A = \frac{\lambda_x\left(\lambda_x^2 - 1\right)}{\left(\lambda_x^2 + 1\right)(W_1 + W_2)} \tag{8}$$

From Eq. (7), the stress ratio in the case of $W_2 = 0$, i.e., with no explicit cross-effect of strains, can be expressed as:

$$\frac{\sigma_y}{\sigma_x} = \frac{\lambda_x}{\lambda_x^2 + 1} \tag{9}$$

The dashed line in Fig. 3a corresponds to Eq. (9). The experimental data at finite strains for all the specimens are located above this line, which indicates that W_2 is finite and positive.

Based on this finding, a new model (extended Gent model) was proposed, which is expressed as the sum of the Gent model and a linear term (I_2):

$$W = \frac{G}{2}\{-(1 - r)(I_\mathrm{m} - 3)\ln(I_1 - 3) + r(I_2 - 3)\} \tag{10}$$

where r is a measure of the contribution of the I_2 term and I_m is the maximum value of I_1, at which the stress becomes infinite. The extended Gent model successfully describes the experimental data over the entire range of λ_x, as shown in Fig. 2d.

Figure 3b shows a plot of r against φ_0 for Tetra gels with various precursor chain lengths. The observed increase in r with increasing φ_0 corresponds to an increase in the coupling effect. The values of r were up to 0.05, which indicates that the contribution from the I_2 term is smaller than that from the I_1 term. Nevertheless, the I_2 term is required to describe the stress–elongation relationship because I_2 becomes substantially larger at moderate and large deformations. The φ_0 dependence of r can be approximated by a linear relation passing through the origin. This result indicates that (1) the magnitude of the cross-effect is governed by φ_0, although it is independent of the network strand length, and (2) no explicit cross-effect is expected at the zero limit of φ_0. In general, φ_0 is defined as the simple polymer concentration during preparation. Conceptually, φ_0

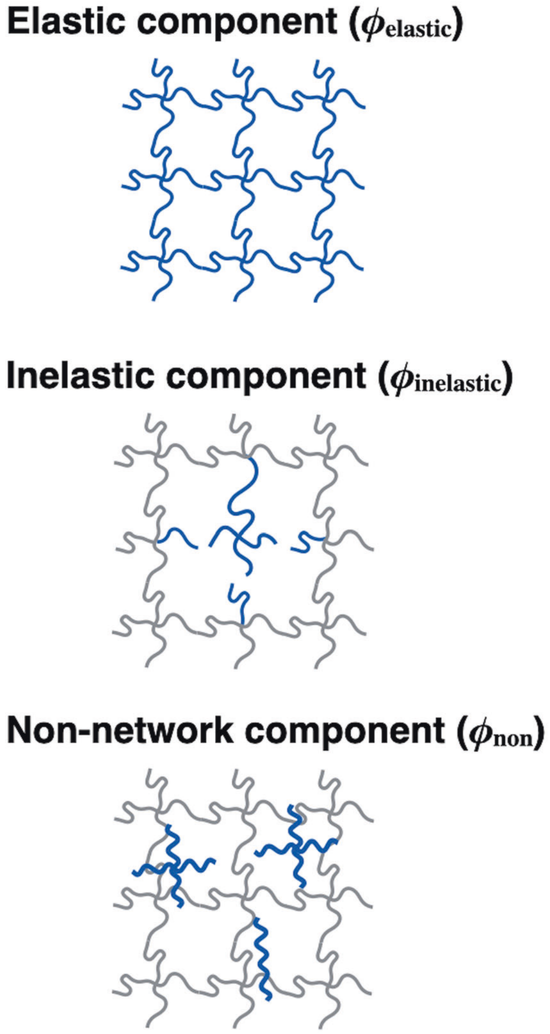

Elastic component (ϕ_{elastic})

Inelastic component ($\phi_{\mathrm{inelastic}}$)

Non-network component (ϕ_{non})

Fig. 4 Schematic illustration of various network substructures: elastic, inelastic, and nonnetwork components

includes the elastic network fraction (elastically effective networks), inelastic network fraction (dangling, loop structures), and non-network fraction (sol fraction), as shown in Fig. 4. To separate these effects, the relationships between r and the fractions of these structures were investigated using connectivity-tuned Tetra gels and Tetra gels with guest chains. It was found that r is governed by the network fraction, which is the sum of the elastic and inelastic network fractions. This result indicates that the cross-effect originates from some interaction between network strands (other than entanglement effects), which is not considered in the classical rubber elasticity models. Several types of interactions have been proposed to account for the deviation of the stress–elongation behavior of crosslinked rubbers from classical theories, such as nematic interactions, which enhance the alignment of neighboring segments, and topological interactions between loop structures in the polymer network. It is difficult to assess the contributions of these two types of interactions to the present biaxial data quantitatively because most models do not provide the analytical form of the stress–elongation relationships required for fitting. Furthermore, the physical meaning of most of the model parameters is qualitative, which makes it difficult to relate the parameters to the structural characteristics of the networks. To elucidate these effects on the mechanical properties of polymer networks, the development of analytical methods accompanied by mechanical properties is desired.

Rheological properties of polymer networks with dynamic crosslinking

Polymer networks with dynamic crosslinks form temporary crosslinking structures through noncovalent bonds, such as ionic interactions, coordinate bonds, hydrogen bonds, and hydrophobic interactions. These networks can be classified into two groups based on their network structures: side-chain and telechelic types, as shown in Fig. 5. This section introduces studies on HG gels and HEUR as representative examples of side-chain-type and telechelic polymer networks, respectively.

Side-chain-type associative polymer networks (HG gels)

HG gels were designed by Harada and coworkers as novel tough soft materials using HG-specific complex formation for crosslinking, as shown in Fig. 6a, to form side-chain-type polymer networks with dynamic crosslinks [8, 27, 28]. HG gels were prepared through the radical polymerization of β-cyclodextrin (βCD)-acrylamide and adamantane (Ad)-acrylamide in addition to conventional vinyl monomers as the main components. βCD and Ad form a stable inclusion complex through hydrophobic interactions, leading to temporary crosslinks in the HG polymer. The HG polymer exhibited high flexibility and outstanding toughness. Furthermore, the HG polymer was easily swollen by water but insoluble in water [29]. In principle, polymer networks with temporary crosslinks cannot reach an equilibrium swollen state because the temporary crosslinks have a finite lifetime. In this case, temporary crosslinks cannot contribute to the elastic free energy at thermal equilibrium. However, contrary to expectations, the HG polymer swelled in water and showed gel-like or solid-like properties. Therefore, the molecular origin of these characteristics of the HG gel was elucidated using rheology and NMR techniques [30].

Figure 6b shows the frequency dependence of the storage and loss moduli (G' and G'') for the HG gel and polyacrylamide (PAA) in solution. For the HG gel, G' and G''

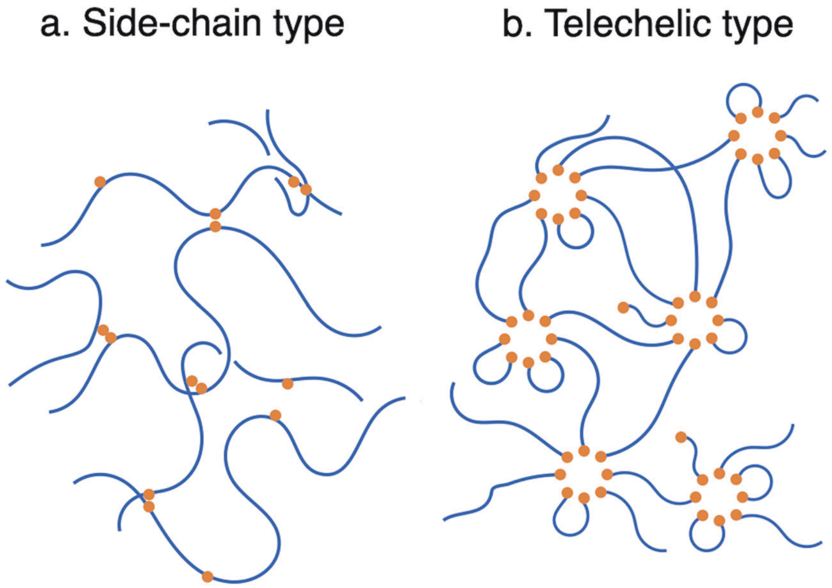

Fig. 5 Classification of polymer networks with dynamic crosslinks: (**a**) associative polymer networks through side-chain interactions (side-chain type) and (**b**) telechelic associative polymer networks (telechelic type)

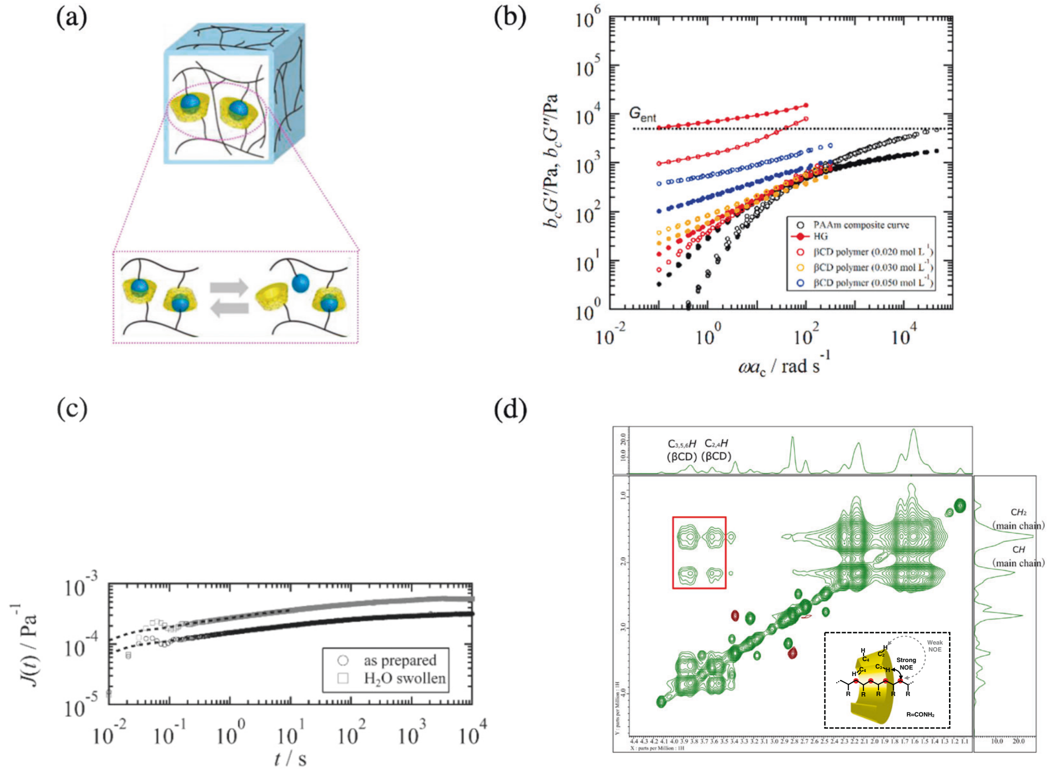

Fig. 6 **a** Schematic illustration of HG gels. **b** Frequency dependences of G′ (open) and G″ (filled) for HG gel, PAA polymers including only βCD groups with different βCD concentrations, and PAA. **c** Creep compliances of HG gel as a function of time. The black circles and gray squares represent *J*(t) for the as-prepared and equilibrium swollen states, respectively. **d** 2D NOESY NMR spectrum of βCD-PAA in D_2O. The red rectangle shows the correlation peaks between CH_2 and CH in the main chains and the H3, 5, 6, and H2, 4 protons of βCD. Reproduced from [30] by permission of the Wiley Online Library

decrease gradually with decreasing ω, and no apparent plateau region is observed for G'. In contrast, the PAA solution shows the typical viscoelastic spectrum of an entangled polymer, with $G' > G''$ at high frequencies and $G'' > G'$ at low frequencies. Interestingly, the rubbery plateau modulus of the PAA solution is identical to that of the HG gel at the low-frequency limit, suggesting that the elasticity of the HG gel is not due to temporary crosslinking but to main chain entanglements. Since the rubbery plateau region of the HG gel was delayed by more than 10^6 times compared with that of the PAA solution, the temporary crosslinks may retard the PAA chain dynamics, allowing the HG gel to flow at a longer time limit. Therefore, creep tests were performed under constant stress to observe the long-term relaxation. Figure 6c shows the creep compliances ($J(t) = \gamma(t)/\sigma$) of the HG gel in the as-prepared and swollen states. $J(t)$ is constant at long times, even in the swollen state, indicating that temporary crosslinks retard the chain dynamics.

To clarify the molecular origin of the unique properties of the HG gel, the role of βCD was examined by investigating the rheology of PAA containing only βCD (Fig. 6b). An increase in the βCD concentration delays the terminal relaxation time, whereas the plateau modulus remains unchanged. This behavior is similar to that of branched entangled polymers [31], suggesting that the addition of βCD causes branching points in the PAA chains. Subsequently, the 2D nuclear Overhauser enhancement (NOE) NMR spectrum was collected for the βCD-PAA solution, as shown in Fig. 6d. The observed cross-relaxation of nuclei between βCD and the PAA main chain suggests that the main chains penetrate the βCDs.

Overall, the obtained data suggest that the HG gel contains two types of crosslinks: dynamic crosslinks resulting from HG interactions and “static” crosslinks resulting from βCD rotaxane structures. The toughness of the HG polymer can be attributed to these “dynamically heterogeneous structures” from the βCD-Ad complex and βCD-rotaxane. The HG inclusion complex works as sticky points to significantly retard segmental and reptation motions. The rotaxane structures between the βCDs and main chains exist and work as permanent crosslinks, which prevents the entire reptation of the chains and makes the terminal relaxation time infinite, resulting in gel-like behavior. Notably, NMR studies have suggested that the βCD molecules in HG gels exist in three states: half of the βCDs form a complex with Ad, less than 1% of the βCDs form a complex with PAAm (penetrating the main chains), and the remaining βCDs do not form any complex. Thus, the contribution of entanglement is dominant in the rubbery plateau. It should be noted that both structures are effective in dissipating elastic energy under larger deformation through the dissociation of the inclusion complexes and the sliding motion of rotaxane-like slide-ring gels.

Telechelic associative polymer networks (HEUR)

A rheological study has been carried out on HEUR in solution as a representative telechelic-type network [32]. HEUR has a hydrophilic main chain with hydrophobic alkyl groups at both ends, as shown in Fig. 7a. The end groups aggregate in water to form temporary crosslinking points, resulting in a network structure. In particular, HEUR composed of nonentangled main chains has been used as a model for dynamic polymer networks because it exhibits a single viscoelastic relaxation [33, 34]. The molecular origin of this single relaxation has been explained by Green and Tobosky [35] and by Yamamoto’s [36] pioneering transient network theory, which assumed that the orientation anisotropy of polymer chains quickly disappears after the aggregation cores collapse, resulting in a single relaxation. However, some deviations from this theory have been reported experimentally. For example, the viscoelastic relaxation time depends on the polymer concentration and molecular weight [37, 38]. Considering these deviations, many attempts have been made to modify the molecular models, such as by introducing the recombination effect. However, these models include some phenomenological fitting parameters, and the molecular mechanism remains unclear.

To understand the molecular origin of the rheological properties, it is essential to monitor the molecular dynamics directly. Therefore, the diffusion behavior of HEUR was evaluated to clarify the relationship between viscoelasticity and diffusion. To assess the diffusivity, fluorescence recovery after photobleaching (FRAP) was utilized. In FRAP measurements, molecules with fluorescent probes in a limited area are exposed to intense light and photobleaching. The self-diffusion coefficient is evaluated according to the time course of intensity recovery owing to the self-diffusion of molecules.

For the FRAP measurements, HEUR modified with fluorescein isothiocyanate (F-HEUR) was synthesized. Figure 7b shows the frequency dependence of G' and G'' for F-HEUR and unmodified HEUR at the same concentration (2 wt%). Both spectra agree with the predictions of the Maxwellian model, as follows:

$$G\prime = G_0 \frac{(\omega\tau)^2}{1+(\omega\tau)^2} \tag{11}$$

$$G\prime\prime = G_0 \frac{\omega\tau}{1+(\omega\tau)^2} \tag{12}$$

where G_0 and τ represent the relaxation strength and time, respectively. This agreement indicates that F-HEUR forms transient networks even after modification. However, G_0 and τ decrease compared with the original values, reflecting the change in the hydrophobic interactions caused by modification.

Subsequently, the viscoelasticity results were compared with the diffusivity using the same F-HEUR sample. Figure 7c shows the relationship between the diffusion

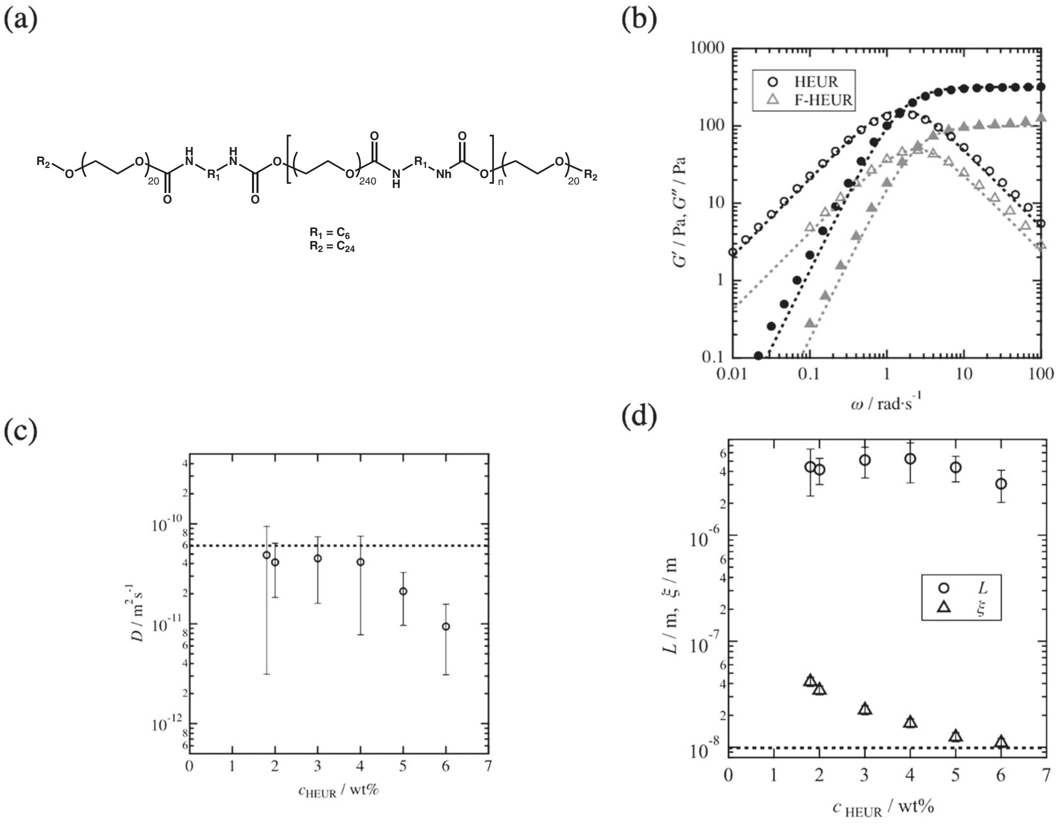

Fig. 7 **a** Chemical structure of HEUR. **b** Frequency dependence of the storage and loss moduli for 2.0 wt% F-HEUR and HEUR solutions. **c** Concentration dependence of the diffusion coefficients calculated from the second-order relaxation times for the F-HEUR solution. The dashed line represents D for a 1.0 wt% HEUR methanol solution, as determined by PFG-NMR measurements. **d** Concentration dependences of the diffusion length during the viscoelastic relaxation time (L) and the effective strand length (ξ) for the F-HEUR solution. The dashed line represents the radius of gyration of the HEUR polymers. Reproduced from [32] by permission of the Japanese Society of Rheology

coefficient (D) and the concentration of F-HEUR. The observed decrease in D with increasing concentration suggests that the HEUR chain dynamics are restricted by the local viscosity or an increase in the number of giant micelles. To clarify the correlation between diffusion and viscoelasticity, the distance that F-HEUR diffused (L) during the viscoelastic relaxation time was estimated. Considering a random diffusion process, L can be written as follows:

$$L = (D\tau)^{\frac{1}{2}} \tag{13}$$

Figure 7d shows the relationship between L and the polymer concentration. The L value is almost constant (≈1 μm), regardless of the polymer concentration. In Fig. 7d, the gyration radius of the HEUR polymers is also shown as a dashed line. The estimated L is more than 100 times larger than the gyration radius, suggesting that HEUR polymers diffuse to a size of ~100 polymers within the viscoelastic relaxation time. Furthermore, L is considerably greater than the distance between the effective crosslinks (ξ), expressed as:

$$\xi = \left(\frac{k_B T}{G_0}\right)^{\frac{1}{3}} \tag{14}$$

These results suggest that there is a significant difference between the diffusion distance and strand length, even at high concentrations.

In a general polymer system, the viscoelasticity originates from the orientational anisotropy of the end-to-end vector [39]. To relax the anisotropy, polymers fluctuate thermally and diffuse a distance roughly equivalent to their own size during the viscoelastic relaxation time. Thus, the observed deviation strongly suggests that the relaxation of HEUR does not originate from the local motion of each chain. Instead, this deviation can be attributed to the dynamic heterogeneity of the network structure, which contains not only superbridge structures but also unimers and flower micelles. In such systems, the network components should diffuse slowly, whereas the unimers and flower micelles should diffuse rapidly.

Although the viscoelastic parameters are sensitive to slow network components, the FRAP measurements may only detect the diffusion of fast components, resulting in a significant difference between L and ξ. This means that some of the molecules incorporated in the network structure can diffuse rapidly through the recombination of the crosslinking cores, for which the recombination rate is much faster than the viscoelastic relaxation time. Based on these results, it is believed that the viscoelastic relaxation of the HEUR network is not primarily determined by the dissociation of the aggregation cores and the diffusion of the HEUR chains.

Conclusion

This review introduces rheological studies on static and dynamic polymer networks. In nonlinear elastic studies on model static networks (Tetra gels), general biaxial stretching revealed the presence of a cross-effect of strains in different directions, even in networks without defects, which is not considered in conventional molecular models. Linear viscoelastic studies on dynamic networks (HG gels and HEUR) accompanied by NMR and FRAP analyses demonstrated that dynamic heterogeneities, such as rotaxane-like crosslinks and micelle structures with different mobilities, strongly influence the rheological properties.

Recently, various types of functional polymer networks with robust toughness and self-healing properties have been designed. These polymer networks are promising materials for many applications, i.e., biomedical, industrial, etc. To utilize these fascinating materials for practical applications, a full understanding of the molecular picture is required. However, interpretation based on limited experiments often leads to an inaccurate understanding. Multiple experimental characterizations, including multiaxial stretching and the combination of dynamic viscoelastic and spectroscopic measurements, will add to the molecular understanding and will further provide important information on the design of novel polymer network materials.

Acknowledgements I thanks to Profs. Sakai and Chung of The University of Tokyo for supervision and Prof. Urayama of Kyoto Institute of Technology and Profs. Inoue, Urakawa, Harada, Takashima, and Nakahata of Osaka University for collaborations. I also thanks to Dr. Kashiwagi and Mrs. Ohnishi of Osaka University for their assistance with experiments. This work was partly supported by the Japan Society for the Promotion of Science (JSPS) through a Grant-in-Aid for Early Career Scientists (grant number: 20K15338).

Compliance with ethical standards

Conflict of interest The author declare no competing interests.

Publisher's note Springer Nature remains neutral with regard to jurisdictional claims in published maps and institutional affiliations.

References

1. Gong JP, Katsuyama Y, Kurokawa T, Osada Y. Double-network hydrogels with extremely high mechanical strength. Adv Mater. 2003;15:1155–8.
2. Okumura Y, Ito K. The polyrotaxane gel: a topological gel by figure-of-eight cross-links. Adv Mater. 2001;13:485–7.
3. Sakai T, Matsunaga T, Yamamoto Y, Ito C, Yoshida R, Suzuki S, et al. Design and fabrication of a high-strength hydrogel with ideally homogeneous network structure from tetrahedron-like macromonomers. Macromolecules. 2008;41:5379–84.
4. Haraguchi K, Takehisa T. Nanocomposite hydrogels: a unique organic–inorganic network structure with extraordinary mechanical, optical, and swelling/de-swelling properties. Adv Mater. 2002;14:1120–4.
5. Yesilyurt V, Webber MJ, Appel EA, Godwin C, Langer R, Anderson DG. Injectable self-healing glucose-responsive hydrogels with pH-regulated mechanical properties. Adv Mater. 2016;28:86–91.
6. Nakahata M, Takashima Y, Harada A. Highly flexible, tough, and self-healing supramolecular polymeric materials using host–guest interaction. Macromol Rapid Commun. 2016;37:86–92.
7. Kakuta T, Takashima Y, Nakahata M, Otsubo M, Yamaguchi H, Harada A. Preorganized hydrogel: Self-healing properties of supramolecular hydrogels formed by polymerization of host–guest-monomers that contain cyclodextrins and hydrophobic guest groups. Adv Mater. 2013;25:2849–53.
8. Nakahata M, Takashima Y, Yamaguchi H, Harada A. Redox-responsive self-healing materials formed from host–guest polymers. Nat Commun. 2011;2:511.
9. Sun TL, Kurokawa T, Kuroda S, Bin Ihsan A, Akasaki T, Sato K, et al. Physical hydrogels composed of polyampholytes demonstrate high toughness and viscoelasticity. Nat Mater. 2013;12:932–7.
10. Yesilyurt V, Ayoob AM, Appel EA, Borenstein JT, Langer R, Anderson DG. Mixed reversible covalent crosslink kinetics enable precise, hierarchical mechanical tuning of hydrogel networks. Adv Mater. 2017;29:1605947.
11. Narita T, Mayumi K, Ducouret G, Hébraud P. Viscoelastic properties of poly(vinyl alcohol) hydrogels having permanent and transient cross-links studied by microrheology, classical rheometry, and dynamic light scattering. Macromolecules. 2013;46:4174–83.
12. Hu J, Hiwatashi K, Kurokawa T, Liang SM, Wu ZL, Gong JP. Microgel-reinforced hydrogel films with high mechanical strength and their visible mesoscale fracture structure. Macromolecules. 2011;44:7775–81.
13. Hu J, Kurokawa T, Nakajima T, Wu ZL, Liang SM, Gong JP. Fracture process of microgel-reinforced hydrogels under uniaxial tension. Macromolecules. 2014;47:3587–94.
14. Gong JP. Why are double network hydrogels so tough? Soft Matter. 2010;6:2583–90.
15. Lane T, Holloway JL, Milani AH, Saunders JM, Freemont AJ, Saunders BR. Double network hydrogels prepared from pH-responsive doubly crosslinked microgels. Soft Matter. 2013;9:7934–41.
16. Liang S, Hu J, Wu ZL, Kurokawa T, Gong JP. Toughness enhancement and stick–slip tearing of double-network hydrogels in poly(ethylene glycol) solution. Macromolecules. 2012;45:4758–63.

17. Na YH, Kurokawa T, Katsuyama Y, Tsukeshiba H, Gong JP, Osada Y, et al. Structural characteristics of double network gels with extremely high mechanical strength. Macromolecules. 2004; 37:5370–4.
18. Nakajima T. Generalization of the sacrificial bond principle for gel and elastomer toughening. Polym J. 2017;49:477–85.
19. Kondo Y, Urayama K, Kidowaki M, Mayumi K, Takigawa T, Ito K. Applicability of a particularly simple model to nonlinear elasticity of slide-ring gels with movable cross-links as revealed by unequal biaxial deformation. J Chem Phys. 2014;141:134906.
20. Kato K, Yasuda T, Ito K. Viscoelastic properties of slide-ring gels reflecting sliding dynamics of partial chains and entropy of ring components. Macromolecules. 2013;46:310–6.
21. Katashima T, Urayama K, Chung U, Sakai T. Probing the cross-effect of strains in non-linear elasticity of nearly regular polymer networks by pure shear deformation. J Chem Phys. 2015;142: 174908.
22. Mayumi K Molecular dynamics and structure of polyrotaxane in solution. Polym J. (2021) https://doi.org/10.1038/s41428-020-00457-9 (in press).
23. Sakai T, Akagi Y, Kondo S, Chung U. Experimental verification of fracture mechanism for polymer gels with controlled network structure. Soft Matter. 2014;10:6658–65.
24. Katashima T, Urayama K, Chung U, Sakai T. Strain energy density function of a near-ideal polymer network estimated by biaxial deformation of Tetra-PEG gel. Soft Matter. 2012;8: 8217–22.
25. Treloar LRG. The physics of rubber elasticity. Oxford: Clarendon Press; 2005.
26. Gent AN. A new constitutive relation for rubber. Rubber Chem Technol. 1996;69:59–61.
27. Harada A, Takashima Y, Nakahata M. Supramolecular polymeric materials via cyclodextrin–guest interactions. Acc Chem Res. 2014;47:2128–40.
28. Sinawang G, Osaki M, Takashima Y, Yamaguchi H, Harada A. Biofunctional hydrogels based on host–guest interactions. Polym J. 2020;52:839–59.
29. Kashiwagi Y, Katashima T, Takashima Y, Harada A, Inoue T. Effect of host-guest interaction on swelling behavior and equilibrium swollen state of host-guest gel. Nihon ReorojiGakkaishi. 2019;47:99–104.
30. Kashiwagi Y, Katashima T, Nakahata M, Takashima Y, Harada A, Inoue T. Linear viscoelastic studies on a transient network formed by host–guest interaction. J Polym Sci Part B Polym Phys. 2018;56:1109–17.
31. Graessley WW, Masuda T, Roovers JEL, Hadjichristidis N. Rheological properties of linear and branched polyisoprene. Macromolecules. 1976;9:127–41.
32. Ohnishi M, Katashima T, Nakahata M, Urakawa O. Relationships between diffusion and viscoelasticity of associative polymer networks. Nihon ReorojiGakkaishi. 2019;47:133–42.
33. Annable T, Ettelaie R. Thermodynamics of phase separation in mixtures of associating polymers and homopolymers in solution. Macromolecules. 1994;27:5616–22.
34. Annable T, Buscall R, Ettelaie R. Network formation and its consequences for the physical behaviour of associating polymers in solution. Colloids Surf A. 1996;112:97–116.
35. Green MS, Tobolsky AV. A new approach to the theory of relaxing polymeric media. J Chem Phys. 1946;14:80–92.
36. Yamamoto M. The visco-elastic properties of network structure I. General formalism. J Phys Soc Jpn. 1956;11:413–21.
37. Uneyama T, Suzuki S, Watanabe H. Concentration dependence of rheological properties of telechelic associative polymer solutions. Phys Rev E Stat Nonlinear Soft Matter Phys. 2012;86:031802.
38. Suzuki S, Uneyama T, Inoue T, Watanabe H. Rheology of aqueous solution of hydrophobically modified ethoxylated urethane (HEUR) with fluorescent probes at chain ends: thinning mechanism. Nihon ReorojiGakkaishi. 2012;40:31–6.
39. Watanabe H. Fundamental findings in soft matter rheology on the basis of multiple methods. Nihon ReorojiGakkaishi. 2013;40: 209–22.

Takuya Katashima received his Ph.D. degree from The University of Tokyo in 2015. His doctoral thesis with Prof. Takamasa Sakai focused on analyzing the nonlinear elasticity of polymer gels using biaxial stretching. He was an assistant professor at Osaka University from 2015 to 2018. After that, he worked as a postdoctoral fellow at RIKEN from 2018 to 2019. He is currently a project assistant professor in the Department of Bioengineering, Graduate School of Engineering, The University of Tokyo. His primary interests are the rheology of polymer networks, including static and dynamic crosslinks.